Are there really superposed Mohos in the southwestern Alps? New seismic data from fan-profiling reflections

F. Thouvenot,[1] A. Paul,[1] J. Fréchet,[1,2] N. Béthoux,[3] L. Jenatton[1] and R. Guiguet[1]

[1] *Laboratoire de Géophysique Interne et Tectonophysique (CNRS/UJF), Maison des Géosciences, BP* 53, 38041 *GRENOBLE CEDEX* 9, *France.*
E-mail: thouve@ujf-grenoble.fr
[2] *Institut de Physique du Globe de Strasbourg (CNRS/ULP),* 5, *rue René-Descartes,* 67084 *STRASBOURG CEDEX, France*
[3] *Géosciences Azur, Sophia-Antipolis,* 250, *rue Albert-Einstein,* 06560 *VALBONNE, France*

SUMMARY

The Moho preserves imprints of the regional geodynamic evolution of the lithosphere. As such, its detailed topography in divergence or convergence zones has a strong bearing on any geodynamic model. This is still more critical where 3-D effects are expected, as in the case of the Alpine chain which exhibits in its western part a short radius of curvature while its trend rotates by 180°. The deep structure of this zone, characterized by a peculiar imbrication of high-density material of lower crust or mantle origin, remains a puzzle. In September 1999, a new controlled-source-seismology experiment was carried out in the southwestern Alps, in the area between the Pelvoux, Dora Maira and Argentera massifs. Five shots were recorded with 130 seismic stations deployed on a total of nine fan- and one in-line profiles. It aimed at getting information on the Moho depth in a hitherto blank area, and discussing the existence of the hypothetical Briançonnais mantle flake mapped in 1986 by the ECORS-CROP experiment. Fan profiles recorded at critical distance for reflections from the European Moho allowed us to map in detail the thickening of the crust from the Mediterranean coastline (27 km) to the root zone (55 km). The zone just south of the Pelvoux massif is characterized by a rather flat, 40-km-deep Moho, which distorts the isobaths in thickening the crust along the Durance valley. Beneath the Argentera massif and just north of it, we evidence a strong dip of the Moho down to 51 km, whereas previous maps predicted depths of 40–46 km only. A new, detailed map of the European Moho can be drawn, which integrates depth data measured at ∼300 reflection midpoints. However, the experiment could not establish the continuity of the Briançonnais mantle flake over a large area in the internal Alps. We observed several reflectors in the 15–31-km depth range. One of them is the Ubaye reflector, a 20-km-long, 23–31-km-deep structure. It might correspond to the Briançonnais mantle flake, although it is located much farther south than the reflector mapped in 1986. New investigations will be necessary to state whether its origin is crustal or due to wedging of mantle material.

Key words: controlled-source seismology, crust, fan profiling, Moho, western Alps, wide-angle reflection.

1 INTRODUCTION

The western Alps (Fig. 1a) are the place where the term 'geologia', introduced in its modern acceptation by the Italian Aldrovandi in the early 17th century, was popularized in the next century by the Swiss Saussure, the first scientist to ascend Mont Blanc in 1787. Since 1956, it has also been a natural test site used by the then nascent experimental seismology. The cooperation framed by the International Geophysical Year brought—in spite of the limited technical capabilities in that time—a large amount of data concerning the deep structure of the western Alps (Closs & Labrouste 1963; Fuchs *et al.* 1963). Mean crustal velocities and estimates of the depth to the

Moho using reflected and refracted waves, mapping of the crustal root beneath the French–Italian border, a seismic study of the Ivrea body—hitherto known from gravity data only—and its interpretation as an upper-mantle wedge produced a wealth of results which really deserves admiration.

In the 1960s and 1970s, controlled-source seismology provided additional details, or confirmed structural hypotheses in different key zones (e.g. Ansorge 1968; Labrouste *et al.* 1968 [hereafter: LBPR68]; Choudhury *et al.* 1971; Perrier 1973; Alpine Explosion Seismology Group 1976; Giese & Prodehl 1976; Ansorge *et al.* 1979). However, decisive progress was achieved in the 1980s when seismic reflection profiling and piggy-back experiments were
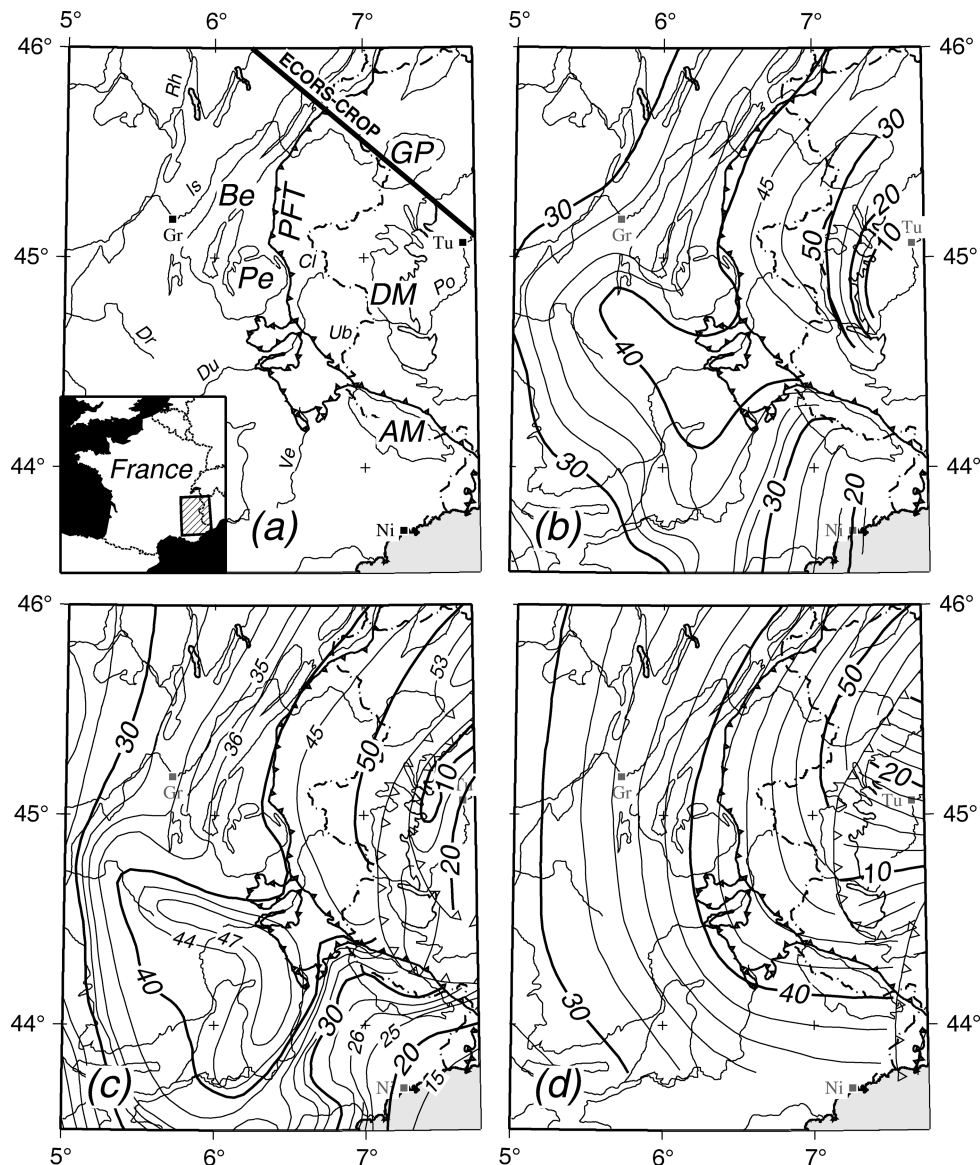
Figure 1. Comparison between three Moho maps in the southwestern Alps. (a) Geographic and tectonic frame, with inset showing position of the study area in the French–Italian Alps. Cities: Gr = Grenoble; Ni = Nice; Tu = Turin. Rivers: Cl = Clarée; Dr = Drôme; Du = Durance; Is = Isère; Rh = Rhone; Ub = Ubaye; Ve = Verdon. Geological units: Be = Belledonne; Pe = Pelvoux; AM = Argentera/Mercantour; DM = Dora Maira; GP = Gran Paradiso; PFT = Penninic Frontal Thrust. ECORS-CROP: position of the cross-section (Fig. 2). (b) M79 Moho map of Ménard (1979), also redrawn by Perrier (1980). (c) GCGP93 Moho map by Grellet *et al.* (1993). (d) WKAM98 Moho map by Waldhauser *et al.* (1998).

carried out in the western Alps as parts of national programmes, such as ECORS (France), CROP (Italy) and NFP/PNR-20 (Switzerland), the results of which were published in three comprehensive volumes (Roure *et al.* 1990, 1996; Pfiffner *et al.* 1997).

In spite of this new wealth of data, information on the deep structure is still sparse in many areas, such as the southern French Alps which essentially remain *terra incognita*. Fig. 1, which shows three different Moho maps for the SE of France, reveals the problem met by authors of syntheses of geophysical data when they addressed this specific point. Ménard (1979) compiled all the seismic profiles available at that time: (1) those from the early experiments from 1956 to 1967 (LBPR68 Moho map); (2) those in the Rhone valley in 1971 and 1972 (Sapin & Hirn 1974); and (3) the 1975 longitudinal profile along the axis of the Alps (Thouvenot & Perrier 1980). Ménard's (1979) map (Fig. 1b) differs from the LBPR68 map in making the

Ivrea body a mantle flake disconnected from the European Moho, beneath the Gran Paradiso and Dora Maira massifs (see isolines 10, 20 and 30 km just west of Turin in Fig. 1b). It also takes into account gravity data in order to reduce the 45-km-deep root introduced by LBPR68 south of the Pelvoux massif. Ménard's (1979) map (hereafter: M79) was redrawn by Perrier (1980). Fig. 1(c) shows a map by Grellet *et al.* (1993) (hereafter: GCGP93). These authors used mainly the same data set and plotted the area between the Pelvoux massif and the Mediterranean coast as a banana-shaped, 47-km-deep crustal root, still deeper than on the original LBPR68 map. Waldhauser *et al.* (1998) were much more conservative, in the sense that they carefully made use of the available data in order to smooth the Moho topography. Their resulting map in Fig. 1(d) (hereafter: WKAM98), may appear somewhat disappointing, because it shows much less detail than the previous ones. However, their processing is
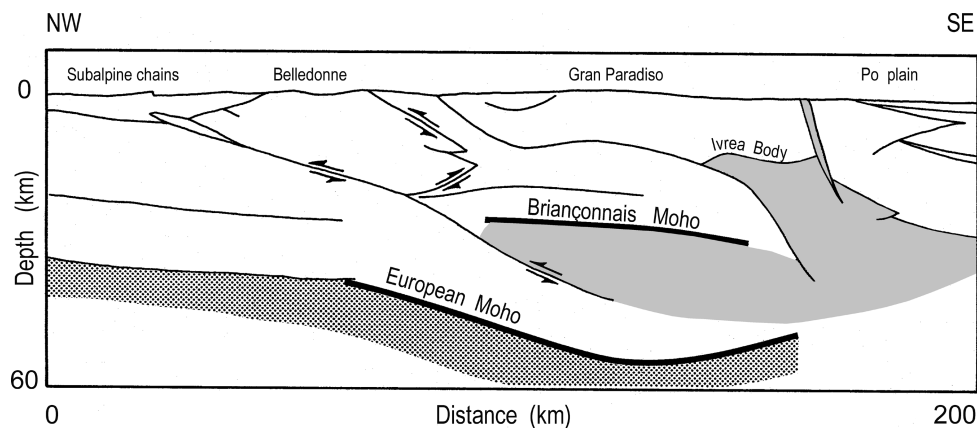
Figure 2. Schematic NW–SE section across the western Alps from the Subalpine chains, NNE of Grenoble, to the Po plain, close to Turin (see position in Fig. 1a). The European (autochthonous) Moho and the Briançonnais (allochthonous) Moho, shown in thick line, both result from the interpretation of the ECORS-CROP wide-angle reflection experiment (EC89). Thin lines are the main seismic discontinuities discovered by the ECORS-CROP seismic reflection profile (after Nicolas *et al.* 1990). The 'Ivrea body' is another shallower mantle flake whose lower contour was re-drawn from Ménard & Thouvenot (1984).

probably sounder. The discrepancies between the three maps mainly result from the lack of data in the southern French Alps.

What has just been said about the European Moho, the position of which cannot be taken for granted in many places, can be even more emphatically stated for other reflectors. More than a decade ago, Kissling (1993) comprehensively discussed existing knowledge of the deep structure of the Alps; indeed it has not evolved much since. An example is provided by one of the main results of the controlled-source-seismology experiment that took place in 1985 as a preliminary to the ECORS-CROP seismic reflection line: the ECORS-CROP Deep Seismic Sounding Group (1989) (hereafter: EC89) discovered, in the root zone, what was interpreted as a mantle wedge intruding the Alpine crust, and extending much farther west than the Ivrea body. To be concise, the upper limit of this 'Briançonnais mantle flake' will be called here 'Briançonnais reflector' (Fig. 2).

This interpretation was grounded on observations along a fan profile recorded in Val d'Aoste (Italy), with a shotpoint in France close to Briançon. A rather low-quality seismic signal was reflected from a 25–30-km-deep discontinuity, while no signal reflected from a deeper Moho could be detected. As the distance between the shotpoint and the fan was larger than 150 km, this interpretation was not clear-cut. However, the ECORS-CROP seismic reflection line (Nicolas *et al.* 1990) confirmed it. In the core of the chain, they observed a highly reflective upper and middle crust which suddenly becomes transparent at around 10 s two-way-time (around 30 km). Since this depth corresponds to that obtained from wide-angle-reflection data, the logical conclusions would be: (1) the wide-angle reflector underlies the highly reflective upper and middle crust; (2) the transparency at greater depth testifies to the presence of upper-mantle material. This viewpoint was supported by a gravity modelling which also requires high-density material in the same place (ECORS-CROP Gravity Group 1989), and adopted in all but two of the subsequent models of the western Alps derived from the ECORS-CROP experiments: Roure *et al.* (1996) and Schmid & Kissling (2000) indeed interpreted the high-density material as duplexes made up of European lower crust.

However, these clues to a flaking of the Alpine lithosphere—a concept Ménard & Thouvenot popularized as early as 1984—were not tangible enough. There was a real need to pursue this key problem, and, when the GéoFrance-3-D programme was launched in

1995 (Groupe de recherche GéoFrance-3-D 1997), its Alps project did include an active-source seismic component.

2 THE EXPERIMENT

2.1 Layout

The backbone of the Moho 99 experiment is a N–S longitudinal profile with two shotpoints: Grand-Saint-Bernard (GSB) in the Grand-Saint-Bernard nappe and Argentera/Mercantour (MER1) in the Argentera/Mercantour crystalline massif (Fig. 3a). This 250-km-long profile runs along the 7°E meridian from Martigny, in the Rhone upper valley, to the Nice hinterland. What looks at first glance an awkward design, with unavoidable offsets when the profile jumps from one valley to another, was conceived in order to get a chance to record refracted waves from the 25–30-km-deep Briançonnais discontinuity, in order to ascertain its mantle origin. We therefore tried to make this profile as long as possible. We assumed that the mantle flake mapped by ECORS-CROP: (1) has a limited lateral extent; (2) has a geometry which follows the general arcuate trend of the western Alps, such as that provided by the Bouguer gravity map (Masson *et al.* 1999) or by the Penninic Frontal Thrust (Fig. 1a). The planned N–S profile could not be placed too far east, because we would then expect to record waves laterally refracted from the Ivrea body (Fig. 2), which would make the interpretation inextricable. Also, the profile could not be made longer by shifting shotpoints farther north and south, because those should not be too far away from the hypothetical mantle flake to allow for a refraction to take place. Altogether, these constraints did not leave much freedom. Both shots were also recorded along two short fan profiles across the chain, with 80 and 100 km observation distances close to the critical distance suitable for mapping this presumed 25–30-km-deep Moho.

Another much longer (270 km) fan profile was also designed to test the existence of the Briançonnais reflector in various parts of the western Alps (Fig. 3b). We used shotpoint Dora Maira (DOM) in the Dora Maira crystalline massif and recorded it at a distance close to 100 km along a wide circle arc which extended from Petit-Saint-Bernard, through Gap, to the Nice hinterland. With this shotpoint–receiver geometry, expected reflection points are situated east of the
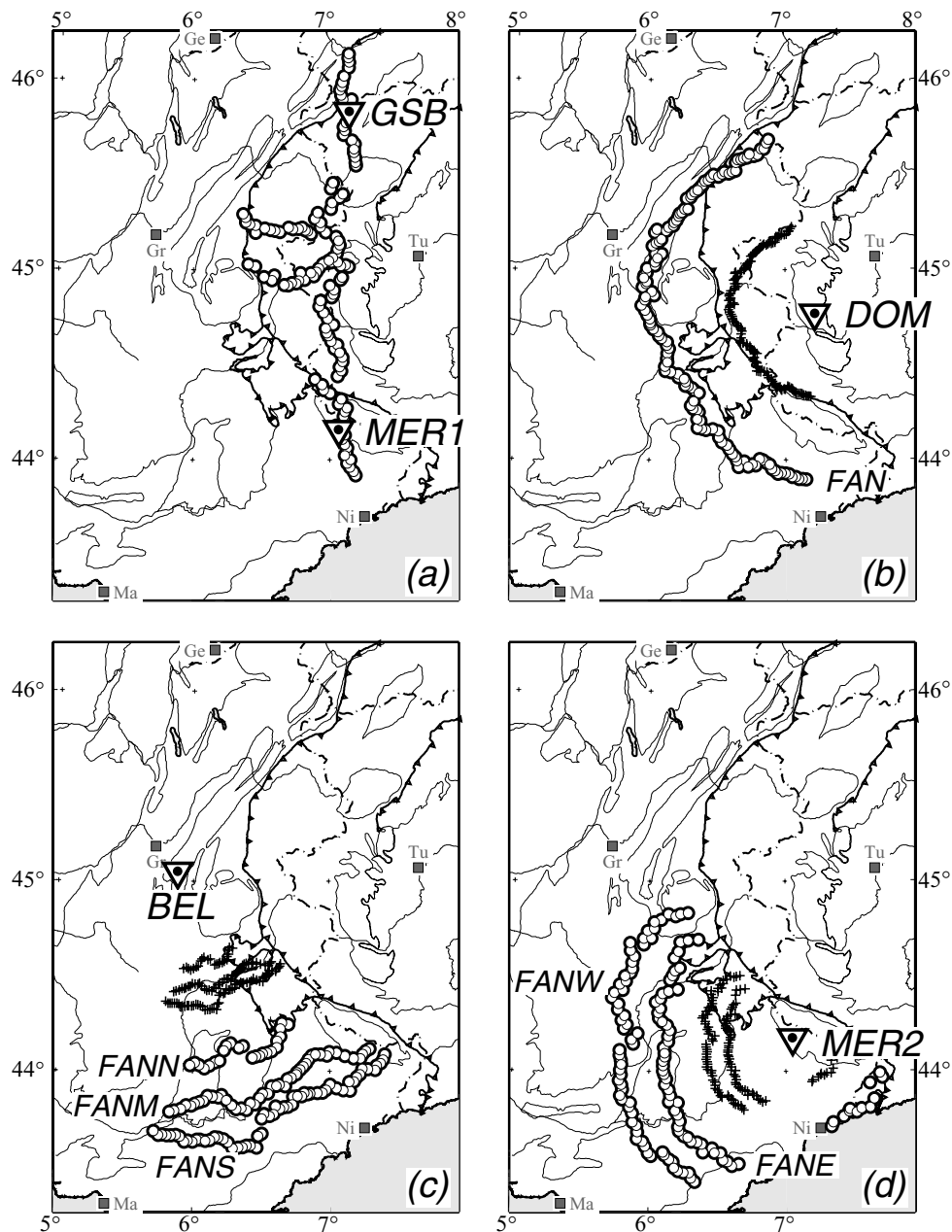
Figure 3. Layout of the Moho 99 active-source seismic experiment. Stations shown by circles, shotpoints by inverted triangles and reflection midpoints for fan profiles by crosses. Cities: Ge = Geneva; Gr = Grenoble; Ma = Marseilles; Ni = Nice; Tu = Turin. (a) Longitudinal profile between Grand-Saint-Bernard (GSB) and Argentera/Mercantour (MER1); (b) fan profile from shotpoint DOM (Dora Maira); (c) fan profiles from shotpoint BEL (Belledonne); (d) fan profiles from shotpoint MER2 (Argentera/Mercantour).

Penninic Frontal Thrust, very close to this main structural feature in the south, much farther inside of the Penninic domain in the north.

Because the position of the European Moho has been mapped only in a few places in the southern French Alps and in Provence, two other shotpoints with multiple-fan recording were devised. Shot Belledonne (BEL), in the Taillefer massif—a splinter massif of the Belledonne crystalline massif—was recorded along three fans totalling 330 km in length and running in a WSW–ENE direction from the Digne nappes to the Nice hinterland (Fig. 3c). Observation distances for the three fans (120, 140 and 160 km) were chosen close to the critical distance suitable for a 40–50-km-deep reflector. Reflection points for such a geometry are indeed located in a

region where previous Moho maps suggested such high values for the Moho depth.

Shot MER2, also fired in the Argentera/Mercantour crystalline massif, was observed along two fans of 160 and 190 km in length, which ran in a N–S direction from Gap to Draguignan (Fig. 3d). With shotpoint–receiver distances of 80 and 100 km, respectively, this geometry is suitable for mapping the European Moho at a depth of about 30 km from the Briançonnais to the Nice hinterland. A very short 40-km-long fan profile was also recorded along the coastline.

Altogether, Moho 99 recorded 1300 km of profiles, with 130 portable receivers, and with station spacing ranging from 2.1 to 3.4 km (Table 1). As such it comprises one of the most intensive

Table 1. Profile characteristics. For fan profiles, Δ is the mean shotpoint–station distance and θ is the aperture angle of the fan as seen from the shotpoint. Shotpoint codes: BEL = Belledonne; DOM = Dora Maira; GSB = Grand-Saint-Bernard; MER = Argentera/Mercantour.

Shotpoint	Profile	Location	Δ (km)	θ (°)	Length (km)	Station #	Spacing (km)
GSB/MER1	LON	Martigny–Vésubie			215	88	2.4
	FANN	Maurienne–Ambin	80	29	40	18	2.4
	FANS	Lautaret–Perosa Argentina	97	32	54	24	2.3
DOM	FAN	Petit-Saint-Bernard–Vésubie	97	161	273	130	2.1
BEL	FANN	Les Mées–Allos	115	31	62	24	2.7
	FANM	Manosque–Vésubie	141	49	121	47	2.6
	FANS	Durance–Gordolasque	159	55	153	59	2.6
MER2	FANS	Beaulieu–Pigna	57	37	37	12	3.4
	FANE	Fréjus–Orcières	82	111	159	53	3.1
	FANW	Maures–Valgaudemar	103	108	194	65	3.0

Table 2. Shotpoint characteristics. Same shotpoint codes as in Table 1.

				Moho 99		
Date	UTC	Shot	Latitude (N)	Longitude (E)	Elevation (m)	Charge (kg)
1999/09/10	19:09:01.663	DOM	44°46.168′	7°13.122′	1370	675
1999/09/13	13:10:57.663	MER2	44°10.496′	7°02.959′	1544	800
1999/09/15	11:10:59.543	BEL	45°03.064′	5°52.821′	1635	1500
1999/09/17	11:00:00.525	MER1	44°09.486′	7°04.057′	1850	1200
	12:21:00.327	GSB	45°49.911′	7°09.856′	2165	800

efforts in controlled-source seismology made during the last decades in the western Alps.

2.2 Shots

In the Alps, EC89 reported that 1000-kg shots could be observed at distances up to 150 km to record waves critically reflected from deep reflectors. Because of the technical limitations related to security rules and access problems, a somewhat lower value (800 kg) was used for most Moho 99 shots, while we planned to load the BEL shot with 1200 kg, because it addressed the deep European Moho. This allowed us to drill only two or three boreholes per shot. Each 8-inch hole was drilled down to approximately 60 m and loaded with a maximum of 400 kg of explosives. Drilling problems allowed us to charge DOM with 675 kg only; the excess explosives that could not be used at DOM were transferred to BEL whose charge was increased to 1500 kg (Table 2). Loading 400 kg per borehole is not really recommended, since it is generally assumed that the shot efficiency increases linearly with the charge up to 200 kg, and in a square-root relation beyond. However, no other solution was available, except perhaps using airlifted drilling equipment which would have given access to more remote outcrops.

2.3 Equipment

We used 130 digital seismic stations borrowed from various French institutions: Parc national de sismique réfraction, Parc national Lithoscope and universities (Grenoble, Nice, Paris). We used a common sampling frequency of 125 Hz and continuous recording.

Stations were equipped with different kinds of three-component seismometers with 2-Hz and 0.2-Hz natural frequencies. Most stations were fed with a GPS time signal receiver; a few of them used a radio-transmitted time signal.

2.4 Signal processing

Recorded signals were converted to SAC (Goldstein 1998) and Sismalp (Fréchet & Thouvenot 2000) formats. Following a Fourier analysis performed on a selection of records, seismograms were systematically bandpass filtered between 1 and 16 Hz. Since we used seismometers with very different natural frequencies, seismograms should have been deconvolved from the instrument response. However, given the low signal-to-noise ratio as well as the uncertainties of the time-to-depth conversion (see next Section), we judged that deconvolution was not critical and decided to use raw (filtered) seismograms. Although the signal-to-noise ratio for reflected *P* waves is higher on the vertical component, we also made use of the horizontal components when possible. Reflections were picked independently on individual seismograms. They were classified into three categories: A (sharp onset), B (medium-quality onset) and C (amplitude increase with unclear onset). This classification was used afterwards to assign a weight to each pick.

3 TIME-TO-DEPTH CONVERSION

The experiment made great use of fan profiles, deliberately ignoring the more usual in-line layouts. Previous studies in the Alps and elsewhere in other orogenic belts (Hirn *et al.* 1980, 1984; EC89; ETH Working Group on Deep Seismic Profiling 1991; Thouvenot *et al.* 1995) indeed demonstrated that fan profiles allowed one to get good value when dealing with Moho topography and reflectivity. Moreover, to be correctly recorded along their total length, in-line profiles demand energetic sources, even more so in the Alps where the crust is highly heterogeneous. Our 800-kg shots were believed to be adequate for wide-angle-reflection studies, with an observation distance close to the critical distance. By trying to record simultaneously in-line profiles, less stations would have been available for fan profiles without providing much useful information.

Table 3. SKTF95 1-D velocity model for the western Alps, with a 38-km-deep Moho.

Depth (km)	Velocity (km s^{-1})
0	4.85
1	5.90
3	5.95
5	6.00
10	6.25
15	6.30
20	6.50
30	6.65
38	8.25
50	8.27
60	8.28

Figure 4. Test of the conversion of a seismogram from the time domain to the depth domain. The SKTF95 velocity model was used to generate a time-dependent seismogram at a distance of 159 km. This seismogram was thereafter converted to the depth-domain by using a 5.95–6.35 km s^{-1} mean crustal velocity in the first 40 km of the crust and the conversion procedure described in the text.

When fan profiles are interpreted, the main problem encountered is the depth conversion of time sections, a problem similar to that faced by near-vertical seismic-reflection profiling. Previous studies usually employed time sections (Hirn *et al.* 1980, 1984; ETH Working Group on Deep Seismic Profiling 1991), with results sometimes flanked by an approximate depth scale. When time sections were converted to depth sections (EC89; Thouvenot *et al.* 1995), this was done for a constant mean crustal velocity, which had to be chosen appropriately.

Values of mean crustal velocity are rare in the western Alps, because one needs long-range inverted in-line profiles to ascertain it. The LBPR68 Moho map was drawn by using the value of 6.07 km s^{-1} for the whole southeast of France; Thouvenot (1976) derived the value of 6.18 km s^{-1} in the north of the western Alps; EC89 used the value of 6.25 km s^{-1}, because the investigated area was more internal to the Alpine arc, where the mean velocity was believed to be higher. A careful review by WKAM98 shows that, although some profiles recorded in the 1960s were inverted, there is a clear lack of reliable velocity data in the southwestern Alps.

Trying to determine a mean velocity over such a wide area might prove hopeless—and also meaningless—because we obviously need a 3-D approach. However, a good starting point would be the 1-D velocity model (Table 3) determined for the western Alps by Sellami *et al.* (1995) (hereafter: SKTF95) from a set of local and regional earthquakes. As most earthquakes are located on the French–Italian border, most seismic rays sample the core of the chain where higher velocities are documented (Paul *et al.* 2001).

To take this into account, we slightly reduced the mean velocity that can be derived from the SKTF95 model between the surface and a reflector at depth for a given observation distance, and modelled it as a velocity increase from 5.90 km s^{-1} at the surface to 6.25 km s^{-1} at a 40-km depth. The latter value ensures a full consistency with the ECORS-CROP processing. Eventually, the time-to-depth conversion was simply performed as follows: starting from the 5.90–6.25 km s^{-1} velocity increase, we computed, for any reflector at depth $z_i = i$ km, the traveltime t_i for the ray emerging at the distance x_0 where the seismogram was recorded. This allowed us to draw up a table of correspondence (z_i, t_i) for that distance. When processing the seismogram, we used this table with linear interpolations in each time-depth interval to plot each sample at proper depth.

Fig. 4 shows a test of the conversion of a synthetic seismogram from the time domain to the depth domain. We fixed the recording distance to 159 km (the largest fan radius, see Table 1), and used the SKTF95 velocity model to generate a time-dependent seismogram. This seismogram was thereafter converted to the depth-domain by
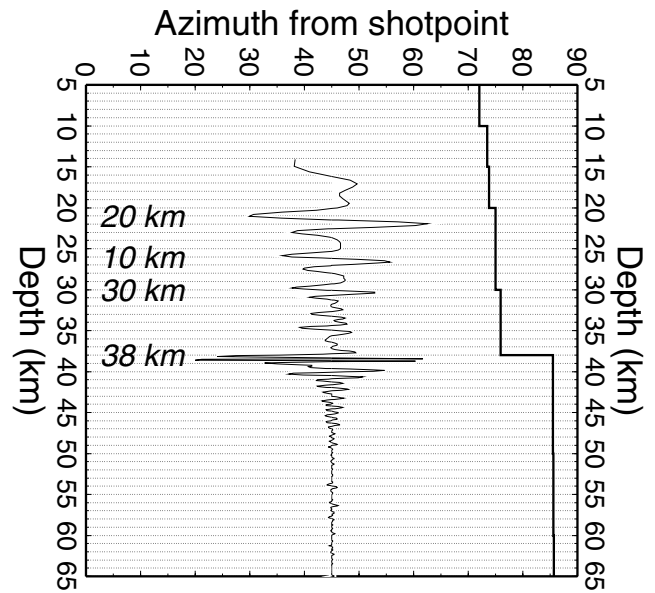
using a 5.95–6.35 km s^{-1} mean crustal velocity in the first 40 km of the crust and the conversion procedure described above. If the conversion were perfect, the depth-converted seismogram should display reflections in agreement with the velocity model on the right.

Deep reflections from the 30-km discontinuity or from the Moho agree fairly well, however, the 20-km discontinuity is displaced by 1–2 km; the 10-km discontinuity provides a reflected signal that is wrongly plotted at a depth of 26–27 km; the 15-km discontinuity cannot be identified. However, it is clear that, although the velocity contrast at 10 km is even larger that at 20 km (Table 3), the recording distance of 159 km is far beyond the 61-km critical distance for the 10-km interface, and closer to the 118-km critical distance for the 20-km interface. Hence, the amplitude of the reflection from the former is smaller than from the latter. As shown by computing traveltime curves, the 140–160 km distance range is also where *traveltimes* for reflections from the upper crust can be larger than from the lower crust. We will have to be cautious when examining and interpreting BEL-FANS and BEL-FANM, two fans recorded in this distance range, where reflections from the upper crust can perhaps spoil the data. At shorter distance (all other fans), this problem will not be normally encountered.

In this study, fan profiles will be presented as depth sections, with each seismogram being plotted vertically along a horizontal axis according to the azimuth of the station (as seen from the shotpoint). In this representation, altitude corrections simply consist in subtracting the mean altitude of the shotpoint and of the station, so that all depths are relative to sea level.

4 EFFECTS OF LATERAL VELOCITY VARIATIONS

The tomographic study by Solarino *et al.* (1997) covers Northwestern Italy, but lacks reliability in the French southwestern Alps which

are on the fringe of their model. Paul *et al.*'s (2001) tomographic study of the region between the Pelvoux, Dora Maira and Argentera massifs only partially covers our study area. Also, most of their model in France is restricted to the first 15 km of the crust, while the largest depth investigated (30 km) is beneath the Po plain. For the time being, it remains therefore difficult to tackle correctly any 3-D velocity variation in the Alpine crust, and we preferred to stick to the 1-D velocity model discussed in the previous section.

However, the technique we used, with a mean crustal velocity increasing with depth, finally allows us to take into account some azimuthal velocity variations, even if, strictly speaking, 3-D structures were not considered. For instance, a ray shot from a given point and reflected from a 30-km-deep Moho will travel in a 6.16 km s^{-1} medium, a value close to that computed by Thouvenot (1976) for the external Alpine domain. In another azimuth, for a 50-km-deep reflector, a 6.34 km s^{-1} value will be used in accordance with what can be computed from the SKTF95 model for the inner part of the chain. Such a velocity increase in the root zone is consistent with the high-density material introduced in existing models, whether implying lower-crust wedging (Roure *et al.* 1996; Schmidt & Kissling 2000) or lithospheric flaking (e.g. ECORS-CROP Gravity Group 1989).

Of course this does not take local velocity anomalies into account. To estimate the corresponding depth uncertainty, we refer to Paul *et al.*'s (2001) tomographic study. In their model, the strongest heterogeneity is the high-velocity Ivrea body, under the Dora Maira massif and the neighbouring Po plain; however, rays shot during our experiment do not sample this structure. The low-velocity anomaly Paul *et al.* (2001) locate in the first 10 km of the crust between the Durance and Verdon rivers is the largest anomaly within our study area. At a 5-km depth, velocities as low as 5.5 km s^{-1} are documented. They correspond to relative velocity variations of ~8 per cent.

However it does not imply that such variations can be expected along a whole ray path. Waves reflected from the Moho sample the entire crust, and it is most likely, from what can be ascertained from Paul *et al.*'s (2001) model where high and low velocity anomalies alternate, that negative and positive traveltime delays will balance. Lateral variations in the mean crustal velocity can be estimated as 5 per cent at the very most. Since precision in velocity and depth are equivalent, it follows that computed Moho depths are here given with a 2-km uncertainty. This value, albeit smaller than the uncertainty introduced by not migrating reflections (see Section 6), is about twice the picking uncertainty, even where onsets are unclear. However, in places where the same Moho reflective element was reached by different ray geometries along different azimuths, Moho depths were averaged. This procedure described in Section 6 will eventually make any lateral velocity variation negligible.

5 THE EUROPEAN MOHO

The three fan profiles originating at shotpoint BEL (Fig. 3c) aimed at providing data for midpoints in a wide area south of the Pelvoux massif, along the Durance upper valley. These profiles are presented in Fig. 5 for the vertical component. Picks are shown as heavy circles with variable radii: large for class-A reflections (sharp onset), small for class-C reflections (amplitude increase with unclear onset). The line drawn across each profile is not just a smoothing of the readings: for each station, the Moho map of Fig. 8—which integrates all the Moho depths provided by this study—was used to compute the 'theoretical' Moho depth at the midpoint. This line, which can thus be considered the 'theoretical' Moho topography along the profile, is useful in places where energy, although present in the signal, has not been used. Picked intracrustal reflections are also shown in Fig. 5 as light circles.

For the vertical component, energy reflected from the Moho is visible on the different fans for different depth ranges: 36–45 km for FANN, 34–45 km for FANM, and 37–49 km for FANS. The N–S and E–W components yield similar values. Altogether, the Moho appears at first glance to be fairly flat in the whole investigated area, with mean values of 41 km south of the Pelvoux massif, 40 km along the Durance valley in the Gap–Embrunais area, and a slightly deeper 44 km on the left bank of the Durance valley in the same area.

We similarly processed the two fan profiles that recorded shot MER2 (Figs 3d and 6). The western fan (FANW) provides the best results, probably because of its larger distance of observation. It demonstrates drastic changes in the quality of the reflections as the distance increases from 80 km (FANE) to 103 km (FANW). All three sections for FANW (Figs 6a–c) show a very clear Moho, which dips from 27 km in the south (with a midpoint beneath the frontal thrust of the Alps in this area, 35 km from the Mediterranean coastline) to 45 km in the north (with a midpoint beneath the Embrunais nappes). This gentle dip is only disturbed by a local high of the Moho topography, around azimuth 240°.

MER2-FANE, with reflection points only 10 km east of those of MER2-FANW, shows a different Moho topography: in Fig. 6d, even if the reflected energy could be picked in a few places only, it is apparent that there is a strong deepening of the Moho in the southern part of the fan, between azimuths 210° and 225°, with a depth increasing from 25 to 35 km over ~10 km of horizontal distance. This is, however, mainly constrained by a few readings only, and by the smoothing of the comprehensive data set presented in Fig. 8. The Moho is then much flatter and reaches a depth of 42 km in the northern part of the fan, beneath the Embrunais nappes.

The fan profile originating at shotpoint DOM (Figs 3b and 7) was aimed at providing many—sometimes redundant—reflection points from the Briançonnais reflector, which will be examined in the next section. Because of its 273-km length, this profile is split in two blow-ups for the vertical component: from due south to due west (Fig. 7a) and from due west to the north (Fig. 7b). Unexpectedly—because the observation distance of ~ 97 km is rather short—the most conspicuous phase is a reflection from a 46–55-km-deep reflector that has to be interpreted as the European Moho. Two processes may explain why such a deep reflected phase could be observed: (1) the westward up-dip of the Moho can help to reduce significantly the critical distance, otherwise computed for a horizontal reflector; (2) a strong velocity contrast across the discontinuity reduces the critical incidence angle, and hence the critical distance. Both processes should be invoked here, because neither alone could explain why this deep Moho, which normally would have its critical distance around 140–160 km by rule of thumb, can be observed at distances shorter than 100 km. The midpoints for these reflections concern the area just north of the Argentera massif (Stura di Demonte valley) where values of 50–52 km are consistently found, the Ubaye nappes (48–50 km), the Briançonnais zone (48–54 km) and the Dora Riparia valley (Susa valley) in Italy (54–55 km). The most intriguing result is the large depth reached by the Moho for midpoints in the Stura di Demonte valley, where previous maps showed values around 45 km only.
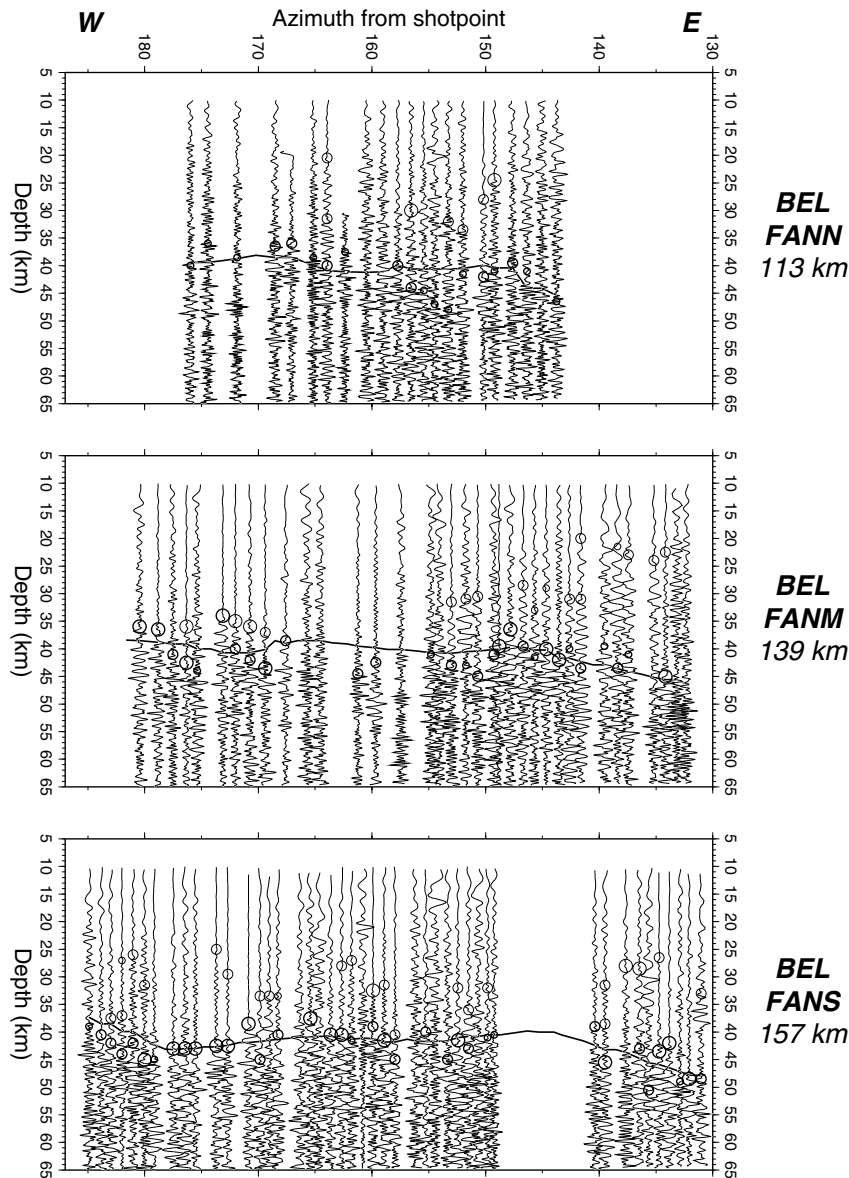
Figure 5. Fan profiles for shotpoint BEL (vertical component), using a 5.90–6.25 km s^{-1} mean crustal velocity in the first 40 km of the crust. (a) Northern fan (FANN); (b) middle fan (FANM); (c) southern fan (FANS). Picks shown as circles (heavy for reflections from the European Moho, light for shallower reflections), with variable radii depending on the quality of the reflection (large = high quality, small = low quality). The line drawn across each profile is not just a smoothing of the readings: for each station, the European Moho map of Fig. 8—which integrates all the Moho depths provided by this study—was used to compute the 'theoretical' Moho depth at the midpoint. This line, which can thus be considered the 'theoretical' Moho topography along the profile, is useful in places where energy, although present in the signal, has not been used. Below record sections, circled letters help to locate reflection midpoints on the map of Fig. 8.

6 A NEW DETAILED MAP OF THE EUROPEAN MOHO

We used the Moho depths picked on all these fan profiles in order to derive a new detailed Moho map for the area 43°45′N–45°12′N and 5°45′E–7°15′E which roughly covers the zone between the Pelvoux, Dora Maira and Argentera crystalline massifs.

First, we plotted all Moho depths onto the map at the midpoint between the shotpoint and the receiver, with weights of 1.0, 0.5 or 0.25 depending on the onset quality on seismograms. By using the GMT software (Wessel & Smith 1998), we superimposed a 10 ×10 km grid onto the map, computed the weighted mean value of depths falling in a given grid cell, and assigned this value to the

cell centre. This processing is necessary to smooth individual values. A new 2 × 2 km grid was then used to compute a continuous curvature surface with a tension factor of 0.35, a value suitable for topographic data (Smith & Wessel 1990). Isobaths for this surface are shown in Fig. 8, with a mask on areas with no data. This limits the investigated area to mainly the Durance and Verdon upper valleys in France, and the Stura di Demonte and Dora Riparia valleys in Italy.

On this map, the general trend is a rather smooth dip of the Moho in a N–S direction, from a depth of 30 km beneath Castellane, 40 km beneath Barcelonnette, 52 km beneath Briançon, down to 55 km beneath the Dora Riparia valley. The Barcelonnette area is a zone where the Moho dip is more pronounced; in the Briançon–Dora Riparia valley area, the crust–mantle discontinuity is much
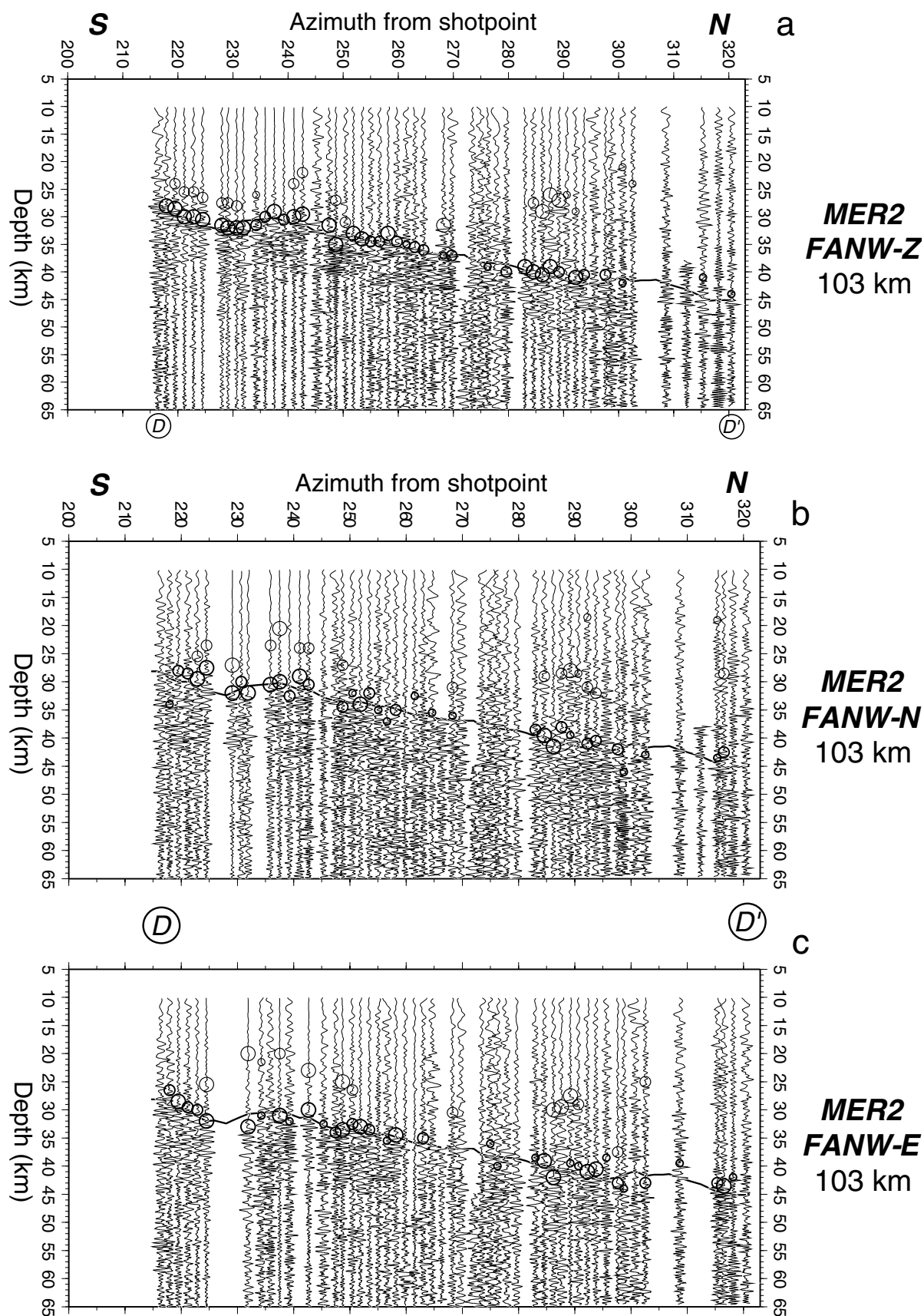
Figure 6. Fan profiles for shotpoint MER2, using a 5.90–6.25 km s^{-1} mean crustal velocity in the first 40 km of the crust. (a) vertical component for the western fan (FANW); (b) and (c) N–S and E–W components for FANW; (d) vertical component for the eastern fan (FANE). See caption to Fig. 5 for a full description.
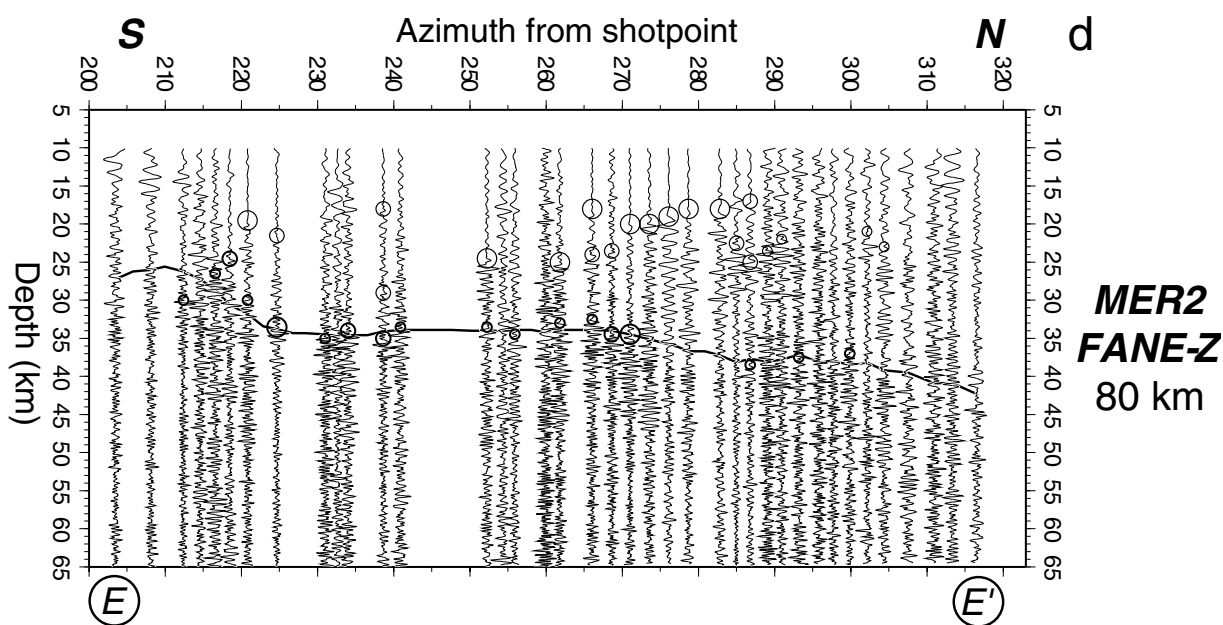
Figure 6. (*Continued.*)

flatter. We note that the value of ∼35 km found in the Digne area is not fully consistent with the 38-km value found in the same place by EC89 (ECORS-CROP shot B, east of Gap, recorded to the south).

Superimposed on this overall N–S dip, the Durance valley, in the centre of the map on the left, is characterized by a significant westward virgation of the 40-km isobath, which makes this zone a kind of shelf with a mean Moho depth of 40 km. This shelf probably extends farther to the west of the study area, since the value of 40 km was also found by EC89 (ECORS-CROP shot A, south of Grenoble, recorded to the south), with reflection points west of Gap (Thouvenot 1996).

In Italy, just north of the Argentera massif, we lack constraints to draw isolines correctly in the Stura di Demonte valley. However, the large values of 50–52 km found in the southern end of the DOM fan profile (Fig. 7a) suggest that there is a drastic increase in crustal thickness across the Argentera massif. Isobaths drawn in this area illustrate this increase without being definitive.

Indeed, the main criticism that can be levelled at the map of Fig. 8 is that Moho depths have been attributed to midpoints between shotpoints and receivers, which is erroneous when the reflector dips. Elementary calculus shows that, in the case of an 11° dip (the maximum dip encountered in the Barcelonnette area), the main effect on a 40-km-deep reflection point is to move it horizontally 25 km updip, while making it 4 km shallower only. A 3-D migration has not been performed here, because we lack at the moment a reliable crustal velocity model in the western Alps, but such a migration is clearly necessary in the future.

7 THE BRIANÇONNAIS REFLECTOR

Shotpoint GSB was located in the phyllites and micaschists of the Grand-Saint-Bernard nappe that belongs to the Briançonnais zone. The drilling was problematical below ∼20 m where cavities and loose material were encountered, although *in-situ* rocks had been recognized at the surface—for this site, as well as for the others. The shot proved inefficient and could be correctly recorded up to 30 km

only. Shotpoint MER1, although located a mere 2.5 km from MER2 which was successful (see Fig. 6), was unfortunately not drilled exactly in the same migmatite outcrop of the Argentera massif. Even with its charge increased to 1200 kg (vs. 800 kg for MER2) MER1 also proved inefficient and could not be recorded beyond 90 km. The corresponding data will therefore not be used in this study. The failure of both shots ruins the evaluation of the seismic velocity at depth along the in-line profile GSB–MER1, and especially that in the hypothetical mantle flake.

However, we had more success with shot DOM for investigating the deep crustal reflectivity over a wide area in the Penninic zone (Fig. 3b). In Fig. 7, in addition to the reflections from the European Moho (heavy circles), we also picked shallower reflections (light circles). Although it is difficult to correlate them from trace to trace, we observe an energy arrival in the 16–31-km depth range along the whole fan. In the 235–255° azimuth range, reflected signals are much more consistent; the depth range narrows and deepens to 23–31 km; we will hereafter refer to this reflector as the Ubaye reflector, since reflection midpoints fall close to the Ubaye upper valley. In the 295–345° azimuth range, energy is reflected from a shallower 16–24-km depth range (Clarée reflector, with reflection midpoints beneath the Clarée valley).

The problem we now face is to interpret these different reflections which apparently sit at different depths. In Fig. 9, we compare a selection of intracrustal reflections in different places: at the top of the figure on the right, the Ubaye reflector; to the left, the Clarée reflector. To be comprehensive, we also show in the lower part of the figure another blow-up of the eastern fan from MER2 where we observe a reflection from the 18–25-km depth range (Verdon reflector, with reflection midpoints beneath the Verdon upper valley). Beneath this reflector, the Moho is 34–37-km deep.

The Verdon reflector is closer to the Alpine foreland. It could as well be the top of a presumably layered lower crust, a characteristic feature of the undeformed European crust in the area (Roure *et al.* 1990, 1996). This lower crust would thicken to the north by the conjunction of the down-dipping Moho and of the up-dipping Verdon reflector.
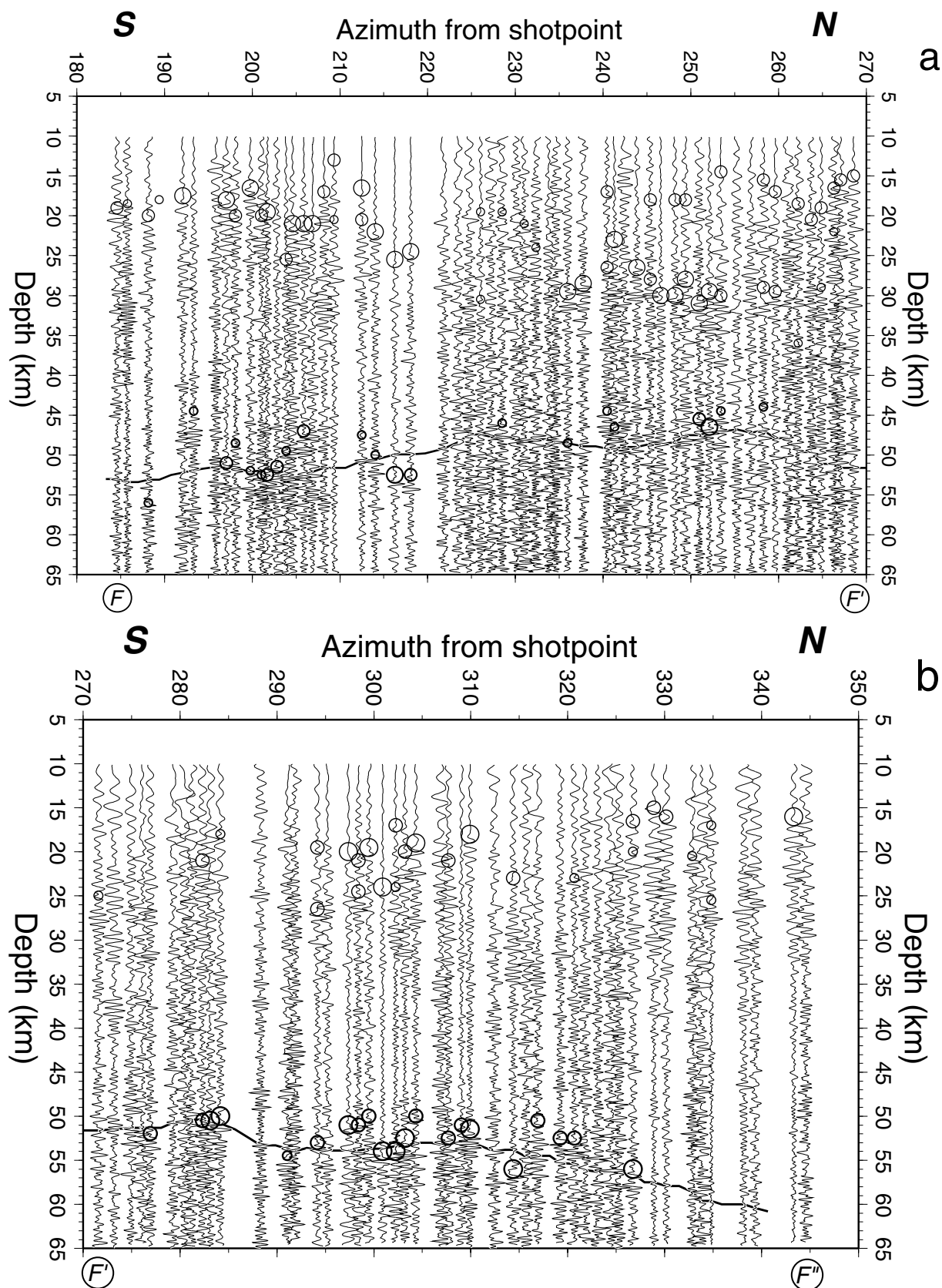
Figure 7. Fan profile for shotpoint DOM (vertical component), using a 5.90–6.25 km s^{-1} mean crustal velocity in the first 40 km of the crust. (a) Southern part; (b) northern part. See caption to Fig. 5 for a full description.
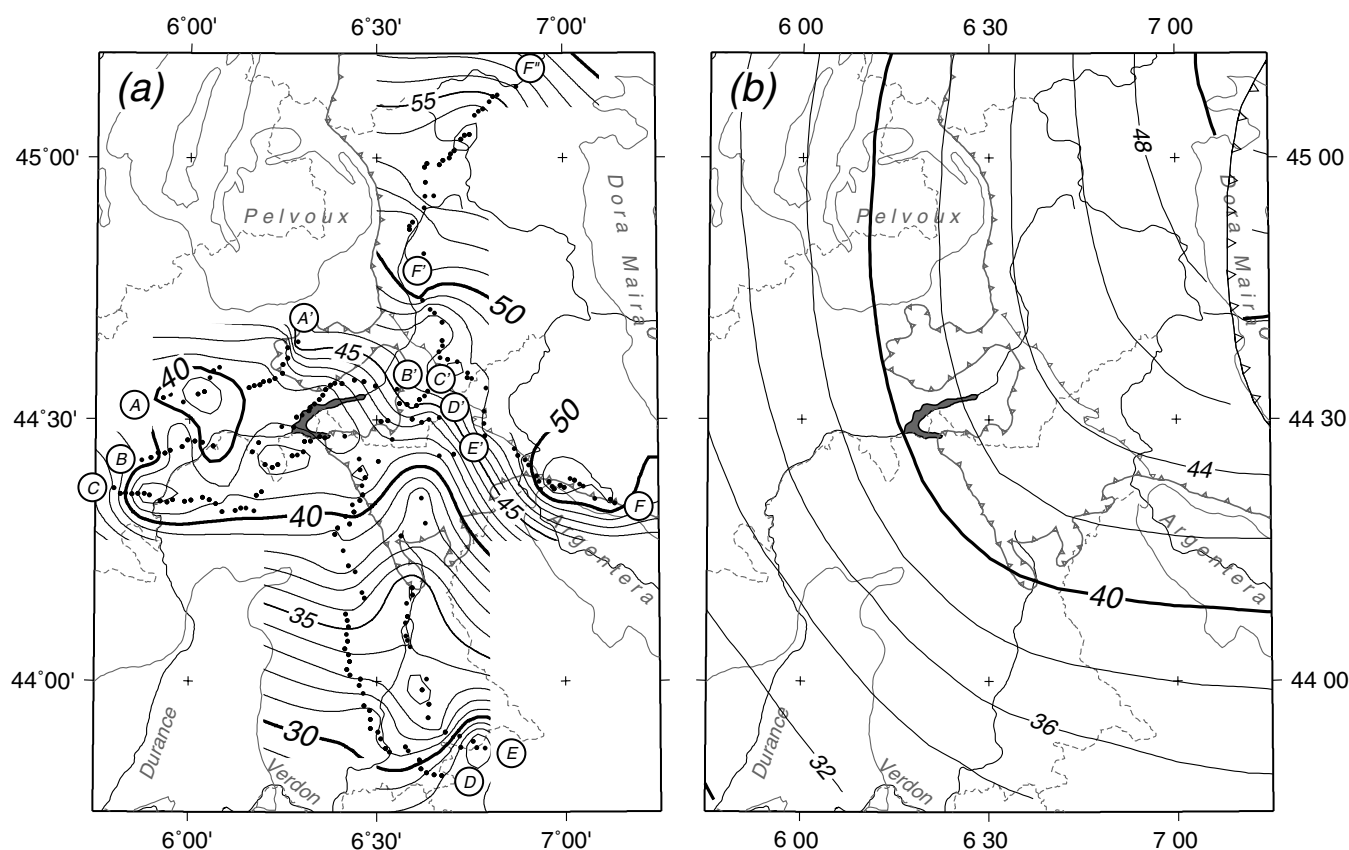
Figure 8. (a) Map of the European Moho beneath the southwestern Alps (unmigrated), using a 5.90–6.25 km skm skm s^{-1} mean crustal velocity in the first 40 km of the crust. Circled letters help to identify, on the record sections of Figs 5, 6 and 7, seismograms which have been used to construct the map. (b) WKAM98 Moho map after Waldhauser *et al.* (1998).

The Clarée reflector cannot have the same origin, unless we admit a 25-km-thick lower crust in the Briançonnais. The sharpness of the reflection from the deep Moho precludes such a thick lower crust. Hence, the Clarée reflector could be either a middle-crust reflector or the Briançonnais Moho evidenced by the ECORS-CROP experiment.

The reflection from the European Moho beneath the Ubaye reflector is very degraded compared to that beneath the Clarée reflector, making the Ubaye reflector very similar to the Briançonnais reflector discovered by EC89 farther north. Therefore, the Ubaye reflector should be likened to the Briançonnais reflector, with a first-order velocity discontinuity marking the top of the mantle flake, or alternatively with a poorly reflective European Moho underneath.

8 DISCUSSION AND CONCLUSIONS

Any tectonic process is likely to leave imprints on the Moho boundary since it is beyond doubt the major seismic marker in the continental lithosphere. The seismic characteristics of that interface, and also its position, topography, smoothness and continuity are amongst many keys that help to unravel the regional geodynamic evolution. For extensional areas in a high heat-flow context, the Moho may migrate, flatten and re-adjust to restore a kind of lateral homogeneity. What happens in regions of tectonic convergence, and especially in the root zones of recent orogens, is much less demonstrable (Ziegler & Dèzes 2006).

In European Alpine orogenic belts, such as the Pyrenees, the central Alps, the northern Apennines or the Dinarides, crustal roots are often related to the insertion of foreland crust into the mantle, with an offset between the upper- and lower-plate Mohos (e.g. Roure *et al.* 1996). The thickness of these crustal roots is variable. For the central Alps, a maximum of 57 km is reached in the Tessino–Engadine region (WKAM98).

The originality of the western Alps is to involve an additional lithospheric flaking which brings mantle material close to the surface, a peculiarity perhaps due to the relatively short radius of curvature of the western Alps ($\sim$100 km) as compared to the total length of the Alpine arc ($\sim$1000 km). This lithospheric flaking is far from being completely understood. Hence, revisiting the Moho topography in the western Alps will provide strong constraints on any Alpine evolutionary model. Marked 3-D effects likely to be induced by the strong arcuate form also require all one's attention.

We showed in this paper that fan profiles recorded at critical distance for reflections from the European Moho allow us to follow the thickening of the crust from the Nice hinterland (27 km) to the root zone (55 km). We measured the Moho depth at about 300 midpoints, for the three shotpoints BEL (Belledonne), MER2 (Argentera/Mercantour), and DOM (Dora Maira) recorded along six fans, with a total length close to 1000 km.

A new Moho map can be drawn, which can be considered provisional, because 3-D migration of reflectors is liable to shift reflection points by up to 25 km from their assumed midpoint positions, while the corresponding depths would be shallowed by a few kilometres.
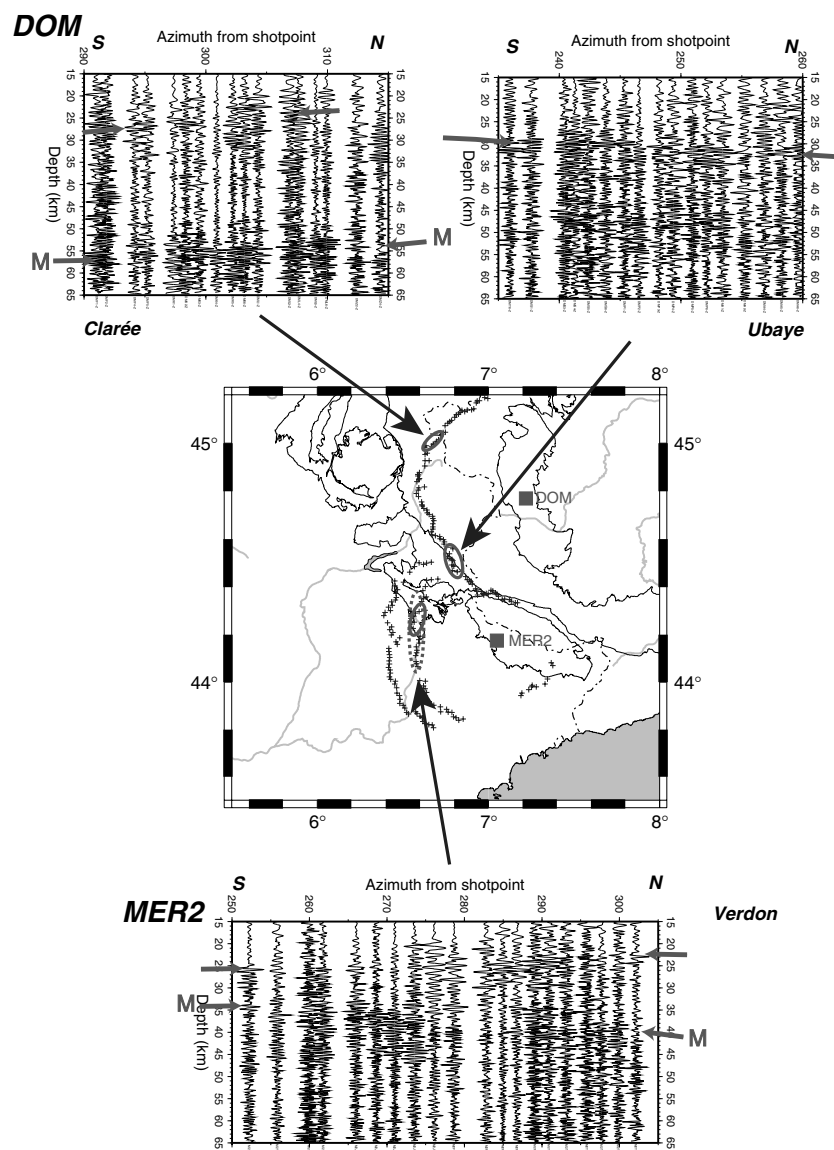
Figure 9. Map showing three blow-ups of the vertical-component cross-sections in three places: (top, left) along DOM-FAN, in the Clarée valley (Clarée reflector); (top, right) along DOM-FAN, in the Ubaye upper valley (Ubaye reflector); (bottom) along MER2-FANE, in the Verdon upper valley (Verdon reflector). The Clarée reflector perhaps links the Ubaye reflector to the Briançonnais reflector evidenced by EC89 farther to the northeast (out of map frame).

However, we do not believe that migration shall provide very different results in the central part of the map, because: (1) the depth to the Moho was measured there using different shotpoint–receiver geometries which provided consistent values; (2) these measurements are in good agreement with those obtained by ECORS-CROP along the southern fans of the wide-angle-reflection seismic experiment (EC89 and Thouvenot 1996), using other shotpoint–receiver geometries. Our unmigrated Moho map will be improved by shooting rays from the different shotpoints, letting them be reflected from a given Moho surface (for instance using the WKAM98 model as a starting point), estimating how traveltimes fit the data, and eventually modifying the surface accordingly. In this direct approach, several rays reflected from different undulations of the Moho could be taken into account and perhaps better explain multiple arrivals. Although such an approach is not straightforward, developing it should be envisaged in the future if we want to overcome the migration problem.

However, the map of Fig. 8 brings information on the Moho depth in a hitherto blank area where previous syntheses showed impressive discrepancies (Fig. 1). The zone that straddles the Durance valley just south of the Pelvoux massif is characterized by a rather flat, 40-km-deep Moho, which distorts the isobaths in thickening the crust along the Durance valley. Curiously, this zone corresponds to a structural saddle: between the Pelvoux and Argentera external crystalline massifs, the basement is depressed, which allowed the transport of the Embrunais-Ubaye nappes to the SW (Kerckhove 1969). On the M79 Moho map, Ménard also drew, south of the Pelvoux massif and along the Durance valley, a similar circumvolution of the 40-km isobath (Fig. 1b). Because the Moho is rather flat in this area, this feature can now be considered well established and we are confident that any subsequent 3-D migration will not alter it.

In the Stura di Demonte valley, just north of the Argentera massif, the large depth of 51 km reached by the Moho is a discovery. Previ-

ous maps predicted depths of at most 40–46 km. Since the Mediterranean coastline is so close to the Argentera massif, it means that the dip of the Moho under that massif is very strong, with the crust thickening by 20 km in less than 30 km in horizontal distance. This thickening cannot be identified on Bouguer anomaly maps, probably because of the presence of the southern end of the shallow, high-density Ivrea body (Masson *et al.* 1999; Vernant *et al.* 2002), which leaves a strong imprint on gravity data. As the Moho topography beneath the Argentera–Stura di Demonte valley is so drastic, reprocessing the data to take migration into account might change isobaths significantly and perhaps reduce the root zone found in that area. We believe, however, that it will not suppress it.

Much farther north, beneath the Dora Riparia valley, we measured a still deeper Moho, down to values of 55 km. In this area, previous maps (M79; GCGP93; WKAM98) provided values of 45 km; for Buness (1992), who plotted 55-km and 60-km isobaths close to Turin, the Moho is somewhat deeper (50 km), but not as deep as what we found. We now have a strong evidence for the crustal root being much thicker, in full agreement with the maximal value of 55 km found by EC89, exactly in this same area, but with a different shotpoint–receiver geometry (shotpoint east of Gap and fan profile across the northern French Alps and the Gran Paradiso massif).

The reliable information provided by Moho 99 on the European Moho makes the contrast with the poor results on the Briançonnais reflector still more striking. One reason is the failure of two shots (MER1 and GSB). Even if these shots had been successful, we might also have had poor results: the fan profile that recorded shot DOM shows that the Briançonnais reflector seems to have such a variable reflectivity that any velocity measurement using refracted waves might be doomed. On that fan, we noted an increase in reflectivity in the 16–31-km depth range. We observed, along a limited, 20-km-long structure, a reflection from the 24–31-km depth range with no clear reflection from the European Moho underneath. The corresponding Ubaye reflector (Fig. 9) lies beneath the Ubaye upper valley, much farther to the south than the Briançonnais reflector mapped by EC89 between the Dora Maira and Gran Paradiso massifs (shotpoint in the Briançonnais zone and fan profile along the Val d'Aoste, Italy). However, in both cases, reflected signals have similar characteristics: unclear onsets, reflectivity in the 24–31-km depth range and no clear reflection from the European Moho underneath. The distance of about 80 km between the Ubaye and Briançonnais reflectors makes their connection hypothetical. However, an intermediate reflector in the 20–25-km depth range (Clarée reflector) could be considered the 'missing link' between them.

The new data demonstrate the high reflectivity observed in the 16–31-km depth range in many parts of the Briançonnais zone, but we could not measure the seismic velocity within this structure, and state whether it is the top of a very thick lower crust or of some mantle wedge. A thick lower crust in the core of the western Alps would fit Schmid & Kissling's (2000) model, which presumes a doubled lower crust in the internal zones, but a joint inversion of local-earthquake traveltimes and gravity data (Vernant *et al.* 2002) confirms a previous gravity modelling by the ECORS-CROP Gravity Group (1989) and demands a high-velocity zone at depths greater than 25 km beneath the internal zones. The consistency with the depth range where the Ubaye, Clarée and Briançonnais reflectors were observed (20–31 km) is remarkable. Since neither the present study nor the joint inversion of Vernant *et al.* (2001) were able to identify the nature of this reflector, it will be a great challenge, in the years to come, to devise new investigation methods to address what finally remains a key problem in the architecture of the Alps.

REFERENCES

Alpine Explosion Seismology Group, 1976. A lithospheric seismic profile along the axis of the Alps, 1975. I: First results, *Pure Appl. Geophys.,* **114,** 1109–1130.

Ansorge, J., 1968. Die Struktur der Erdkruste an der Westflanke der Zone von Ivrea, *Schweiz. Min. petr. Mitt.,* **48,** 235–246.

Ansorge, J., Mueller, S., Kissling, E., Guerra, I., Morelli, C., & Scarascia, S., 1979. Crustal section across the zone of Ivrea-Verbano from the Valais to the Lago Maggiore, *Boll. Geofis. Teor. Appl.,* **21,** 149–157.

Buness, H., 1992. Krustale Kollisionsstrukturen an den Rändern der nordwestlichen Adriaplatte, *Diss.*, Fr. Univ. Berlin, p. 221.

Choudhury, M.A., Giese, P. & de Visintini, G., 1971. Crustal structure of the Alps: some general features from explosion seismology, *Boll. Geofis. Teor. Appl.,* **13,** 211–240.

Closs, H. & Labrouste, Y., 1963. *Recherches séismologiques dans les Alpes occidentales au moyen de grandes explosions en 1956, 1958 et 1960, Mém. Coll. Année géophys. Int.,* **12,** p. 241.CNRS, Paris.

ECORS-CROP Deep Seismic Sounding Group, 1989. Mapping the Moho of the western Alps by wide-angle reflection seismics, *Tectonophysics,* **162,** 193–202.

ECORS-CROP Gravity Group, 1989. Gravity modelling along the ECORS-CROP vertical seismic reflection profile through the western Alps, *Tectonophysics,* **162,** 203–218.

ETH Working Group on Deep Seismic Profiling, 1991. Integrated analysis of seismic normal incidence and wide-angle relection measurements across the eastern Swiss Alps. In: Meissner, R., Brown, L., Dürbaum, H.-J., Franke, W., Fuchs, K. & Seifert, F. (eds), *Continental*

Lithosphere: Deep Seismic Reflections, *Geodyn. Ser.*, Vol. **22**, pp. 195–205.

Fréchet, J. & Thouvenot, F., 2000. Pickev2000, http://sismalp.obs.ujf-grenoble.fr/ftp-sismalp/msdos

Fuchs, K., Mueller, S., PeterSchmitt, É., Rothé, J.-P., Stein, A. & Strobach, K., 1963. Krustenstruktur der Westalpen nach refraktionsseismischen Messungen, *Beitr. Geophys.,* **72,** 149–169.

Giese, P. & Prodehl, C., 1976. Main features of crustal structure in the Alps. In: Giese, P., Prodehl, C., Stein, A. (eds), *Explosion Seismology in Central Europe. Data and Results*, p. 429, Springer, Berlin.

Goldstein, P., 1998. SAC2000, http://www.llnl.gov/sac

Grellet, B., Combes, P., Granier, T. & Philip, H., 1993. Sismotectonique de la France métropolitaine dans son cadre géologique et géophysique, *Mém. Hors-Sér. Soc. géol. Fr.,* **164,** 1–75.

Groupe de recherche GéoFrance 3D, 1997. GéoFrance 3D: l'imagerie géologique et géophysique du sous-sol de la France, *Mém. Soc. géol. France,* **172,** 53–71.

Hirn, A., Daignières, M., Gallart, J. & Vadell, M., 1980. Explosion seismic sounding of throws and dips in the continental Moho, *Geophys. Res. Lett.,* **7,** 263–266.

Hirn, A. *et al.*, 1984. Crustal structure and variability of the Himalayan border of Tibet, *Nature, Lond.,* **307,** 23–25.

Kerckhove, C., 1969. La 'zone du Flysch' dans les nappes de l'Embrunais-Ubaye (Alpes occidentales), *Géol. Alp.,* **45,** 5–204.

Kissling, E., 1993. Deep structure of the Alps: What do we really know?, *Phys. Earth Planet. Int.,* **79,** 87–112.

Labrouste, Y., Baltenberger, P., Perrier, G. & Recq, M., 1968. Courbes d'égale profondeur de la surface de Mohorovicic dans le Sud-Est de la France, *C. r. Acad. Sc., Paris,* **266,** 1530–1533.

Masson, F., Verdun, J., Bayer, R. & Debeglia, N., 1999. Une nouvelle carte gravimétrique des Alpes occidentales et ses conséquences structurales et tectoniques, *C. R. Acad. Sci., Paris,* **329,** 865–871.

Ménard, G., 1979. Relations entre structures profondes et structures superficielles dans le Sud-Est de la France. Essai d'utilisation de données géophysiques, *Thesis*, Grenoble.

Ménard, G. & Thouvenot, F., 1984. Écaillage de la lithosphère européenne sous les Alpes occidentales : arguments gravimétriques et sismiques liés à l'anomalie d'Ivrea, *Bull. Soc. géol. Fr.,* **26,** 875–884.

Nicolas, A., Polino, R., Hirn, A., Nicolich, R. & ECORS-CROP Working Group, 1990. Lithospheric wedging in the western Alps inferred from the ECORS-CROP traverse, *Geology,* **18,** 587–590.

Paul, A., Cattaneo, M., Thouvenot, F., Spallarossa, D., Béthoux, N. & Fréchet, J., 2001. A three-dimensional crustal velocity model of the southwestern Alps from local earthquake tomography, *J. Geophys. Res.,* **106,** (19), 367–19.

Perrier, G., 1973. Structure profonde des Alpes occidentales et du Massif central français, *Thèse d'État*, Paris.

Perrier, G., 1980. La structure des Alpes occidentales déduite des données géophysiques, *Eclog. geol. Helv.,* **73,** 407–424.

Pfiffner, O.A., Lehner, P., Heitzmann, P., Mueller, S. & Steck, A., 1997. *Deep structure of the Swiss Alps: results of NRP 20*, p. 380, Birkhäuser, Basle.

Roure, F., Heitzmann, P. & Polino, R., 1990. Deep structure of the Alps. *Mém. Soc. géol. Fr., Paris,* **156**; *Mém. Soc. géol. Suisse, Zurich,* **1**; *Vol. spec. Soc. Geol. It., Rome,* **1,** 350.

Roure, F., Bergerat, F., Damotte, B., Mugnier, J.-L. & Polino, R., 1996. The ECORS-CROP Alpine seismic traverse. *Mém. Soc. géol. Fr., Paris,* **170,** 113 p.

Roure, F., Choukroune, P. & Polino, R., 1996. Deep seismic reflection data and new insights on the bulk geometry of mountain ranges, *C. R. Acad. Sc. Paris,* **322,** 345–359.

Sapin, M. & Hirn, A., 1974. Results of explosion seismology in the southern Rhone valley, *Ann. Géophys.,* **30,** 181–202.

Schmid, S. & Kissling, E., 2000. The arc of the western Alps in the light of geophysical data on deep crustal structure, *Tectonics,* **19,** 62–85.

Sellami, S., Kissling, E., Thouvenot, F. & Fréchet, J., 1995. Initial reference velocity model for seismic tomography in the western Alps (Poster). *20th Gen. Ass. Europ. Geophys. Soc.*, Hamburg.

Smith, W.H.F. & Wessel, P., 1990. Gridding with continuous curvature splines in tension, *Geophysics,* **55,** 293–305.

Solarino, S., Kissling, E., Sellami, S., Smriglio, G., Thouvenot, F., Granet, M., Bonjer, K.P. & Sleijko, D., 1997. Compilation of a recent seismicity data base of the greater Alpine region from several seismological networks and preliminary 3-D tomographic results, *Ann. Geofis.,* **XL,** 161–174.

Thouvenot, F., 1976. Sondages sismiques profonds Alpes 75. Premiers résultats sur la structure de la lithosphère entre les massifs du Revard (France) et du Gothard (Suisse). *Dipl. Ing.-Géophys.*, Strasbourg.

Thouvenot, F., 1996. Aspects géophysiques et structuraux des Alpes occidentales et de trois autres orogènes Atlas, Pyrénées, Oural). *Thèse d'État*, Grenoble.

Thouvenot, F. & Perrier, G., 1980. Seismic evidence of a crustal overthrust in the western Alps, *Pageoph,* **119,** 163–184.

Thouvenot, F., Kashubin, S.N., Poupinet, G., Makovskiy, V.V., Kashubina, T.V., Matte, P. & Jenatton, L., 1995. The root of the Urals: evidence from wide-angle reflection seismics, *Tectonophysics,* **250,** 1–13.

Vernant, P., Masson, F., Bayer, R. & Paul, A., 2002. Sequential inversion of local earthquake traveltimes and gravity anomaly—The example of the western Alps, *Geophys. J. Int.,* **150,** 79–90.

Waldhauser, F., Kissling, E., Ansorge, J. & Mueller, S., 1998. Three-dimensional interface modelling with two-dimensional seismic data: the Alpine crust–mantle boundary, *Geophys. J. Int.,* **135,** 264–278.

Wessel, P. & Smith, W.H.F., 1998. New, improved version of Generic Mapping Tools released, *EOS Trans. Am. Geophys. Un.,* **79,** 579.

Ziegler, P.A. & Dèzes, P., 2006. Crustal evolution of western and central Europe. in Gee, D. & Stephenson, R. A. (eds), *European Lithosphere Dynamics*, *Geol. Soc., London, Mem.*, **32,** pp. 43–56.